CHEMBIOCHEM

Supporting Information

CHEMBIOCHEM

Supporting Information

for

Two-Photon Fluorescent Probes for Biomembrane Imaging: Effect of Chain Length

Hwan Myung Kim, Bo Ra Kim, Hyo-Jung Choo, Young-Gyu Ko, Seung-Joon Jeon, Chul Hoon Kim, Taiha Joo,* and Bong Rae Cho*

Table of Contents

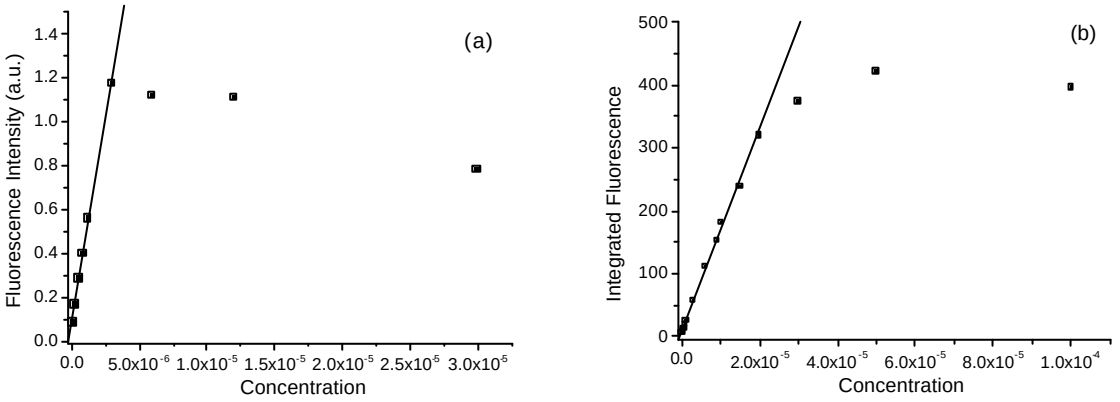

Figure S1. Plot of fluorescence intensity against dye concentration for a) C-hexadan (CH) and b) C-laurdan (CL) in H_2O. The excitation wavelength was 365 nm. The water solubility of C-steardan (CS) was not determined. The fluorescence intensity was too weak to measure the solubility in H_2O.

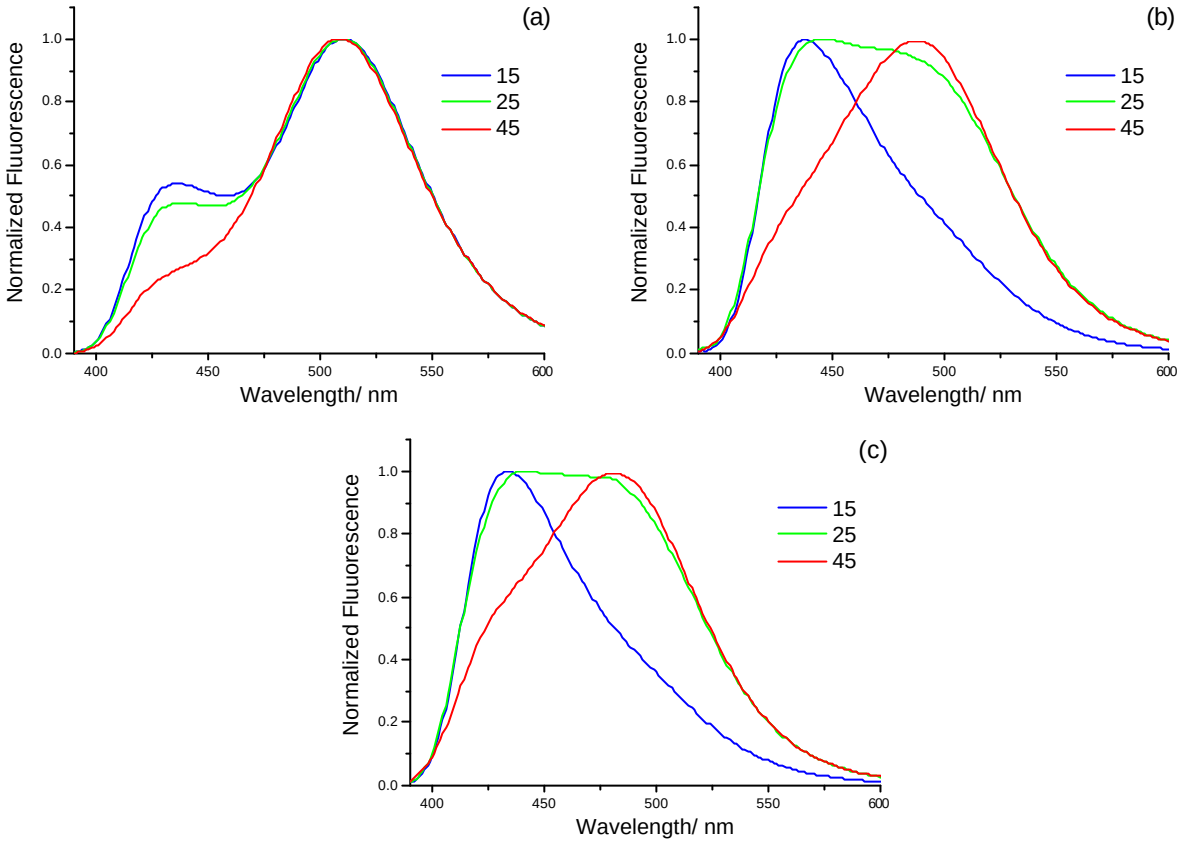

Figure S2. Emission spectra of a) CH, b) CL, and c) CS in the phospholipid vesicles composed of DOPC/sphingomyelin/cholesterol (Raft mixture, 1:1:1) at 15, 25, and 40 ± 0.5 °C, respectively. Excitation wavelength is 365 nm.

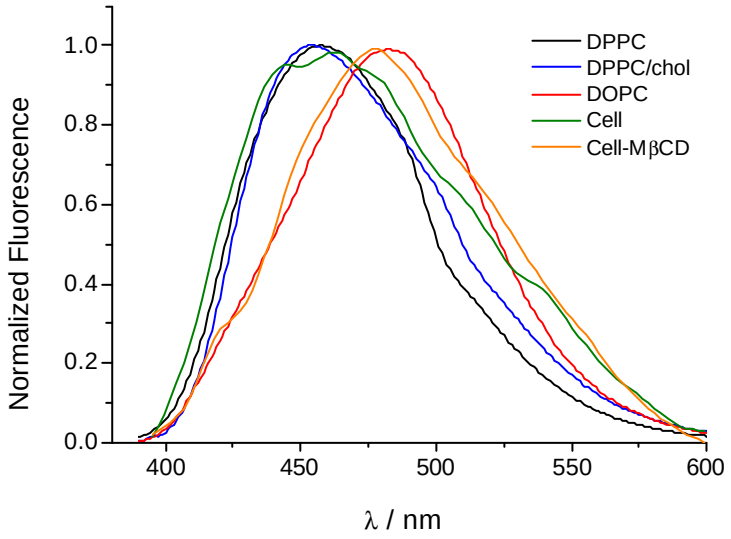

Figure S3. Normalized emission spectra of CS in the phospholipid vesicles composed of DPPC (black), DPPC/cholesterol (DPPC/chol, chol 40 mol%, blue) and DOPC (red), and CS-labeled 293T cell before (green) and after (orange) treatment with 10 mM MβCD for 30 min.

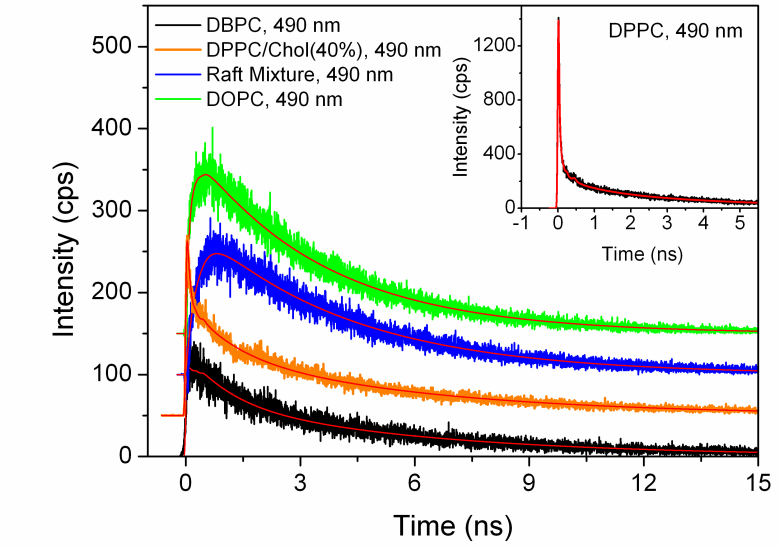

Figure S4. Picosecond time resolved fluorescence of the C-steardan in vesicles. Excitation wavelength is 380 nm. The curves are displaced in y axis for clarity.

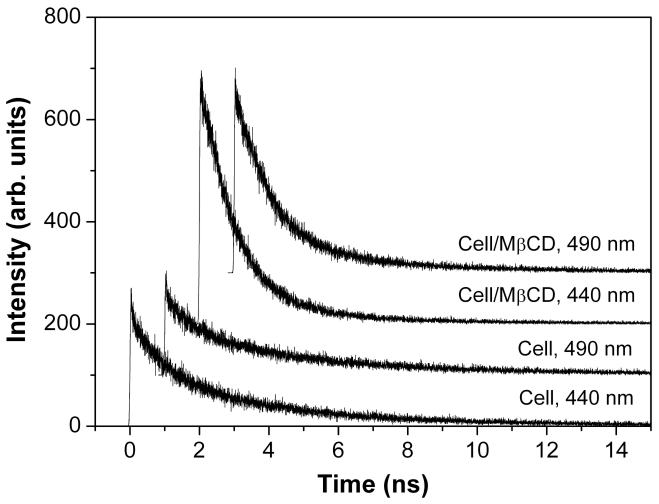

Figure S5. Picosecond time resolved fluorescence of the CS in cells. Excitation wavelength is 380 nm. The curves are displaced in *x* and *y* axes for clarity.

Temperature-dependent TRF experiments for the CH, CL, and CS in two different raft mixtures were performed. Figure S3 and S4 show TRF signals of each probe in the raft mixture (1:1:1) and (2:2:1), respectively. Their multi-exponential fitting results are listed in Table S2 and S3, respectively. For all the raft mixtures, the TRFs of each probe clearly follow their temperature dependent stationary spectra shown in Figure S2. At low temperature (15 $^{\circ}$C), any rise components at 490 nm weren't detected for

all mixtures, but at high temperature (45 °C), a rise of the ICT band were probed for the CL and CS, indicating that both raft mixtures are dominantly in gel phase at 15 °C, but they are in liquid crystal phase at 45 °C. The TRFs performed at room temperature (25 °C) can be well described in terms of a sum of two different lipid phase contributions.

Table S1. Multiexponential nonlinear least square fit results for the time resolved fluorescence of CS in vesicles and cells. Vesicles themselves show a small fluorescence, which appears as an ultrafast 27 ps component in the TRF (see Figure S4). This contribution was subtracted by measuring the TRF of the unstained vesicles.

	λ (nm)	A_1	τ_1 (ps)	A_2	τ_2 (ns)	A_3	τ_3 (ns)
DBPC	440			0.43	1.7	0.57	5.6
	490			0.45	1.0	0.55	5.7
DPPC	440	0.65	92	0.20	0.89	0.15	4.5
	490	0.74	92	0.11	1.1	0.15	4.6
DPPC/ Chol(40%)	440	0.41	129	0.35	2.6	0.24	6.9
	490	0.56	92	0.18	1.1	0.26	5.6
Raft mixture	440			0.51	1.3	0.49	4.3
	490	-0.5	240			0.50	4.0
DOPC	440			0.57	0.55	0.43	2.4
	490	-0.50	90			0.50	3.4
Cell	440	0.32	100	0.38	1.0	0.30	4.3
	490	0.38	78	0.31	0.93	0.31	4.6
Cell/MβCD	440			0.84	0.79	0.16	2.5
	490			0.81	0.82	0.19	3.4

Table S2. Multiexponential nonlinear least square fit results for the temperature dependent TRF of CH, CL, and CS in Raft mixture (1:1:1).

	λ (nm)	*T* (°C)	A_1	τ_1 (ps)	A_2	τ_2 (ns)	A_3	τ_3 (ns)
C-Hexadan	440	15	0.29	161	0.38	1.9	0.34	5.6
		25	0.40	58	0.31	1.1	0.29	4.2
		45	0.79	6	0.10	7.2	0.11	3.2
	490	15			0.79	1.4	0.21	3.4
		25			0.79	1.1	0.21	3.0
		45			0.81	0.73	0.19	2.5
C-Laurdan	440	15	0.88	5	0.05	0.98	0.07	5.2
		25	0.92	6	0.03	0.76	0.04	4.2
		45	0.29	78	0.35	0.88	0.36	3.1
	490	15			0.04	0.26	0.96	5.0
		25			0.26	0.27	0.74	4.4
		45			-0.21	0.33	0.79	3.4
C-Steardan	440[1]	15	0.98	0.16	0.007	0.85	0.01	4.9
		25	0.99	0.10	0.005	0.51	0.01	3.7
		45	0.83	8	0.08	0.42	0.08	2.5
	490	15			0.18	0.38	0.82	4.9
		25			0.36	0.26	0.64	4.0
		45			-0.18	0.74	0.82	3.6

[1] Some portion of the first decay component of the TRF monitored at 440 nm originated from the vesicle. Raft mixture (1:1:1) itself showed a small fluorescence at 440 nm, which appears as an ultrafast decay that is similar to the instrument response.

Table S3. Multiexponential nonlinear least square fit results for the temperature dependent TRF of CH, CL, and CS in Raft mixture (2:2:1).

	λ (nm)	T (^{o}C)	A_1	τ_1 (ps)	A_2	τ_2 (ns)	A_3	τ_3 (ns)
C-Hexadan	440	15	0.35	87	0.38	1.2	0.27	4.7
		25	0.58	20	0.24	0.73	0.18	3.6
		45	0.82	6	0.10	0.62	0.08	2.9
	490	15			0.74	1.4	0.26	3.2
		25			0.71	1.1	0.29	2.7
		45			0.81	0.76	0.19	2.4
C-Laurdan	440	15	0.42	52	0.28	1.2	0.30	5.9
		25	0.37	88	0.36	1.2	0.27	5.2
		45	0.37	96	0.39	0.78	0.24	3.1
	490	15			0.70	3.2	0.30	6.5
		25	0.13	102	0.79	3.4	0.08	8.1
		45	-0.14	266	0.68	2.1	0.19	4.5
C-Steardan	440[1]	15	0.99	0.11	0.004	0.48	0.004	3.6
		25	0.99	0.16	0.005	0.39	0.004	3.1
		45	0.98	0.13	0.014	0.34	0.010	2.5
	490	15	0.60	166	0.26	0.14	0.14	5.1
		25	0.38	61	0.30	0.39	0.33	3.7
		45	0.16	65			0.84	3.7
	540[2]	45			-0.19	0.95	0.81	3.8

[1] Some portion of the first decay component of the TRF monitored at 440 nm originated from the vesicle.

[2] A rise component for the ICT emssion was clearly resolved at 540 nm because of negligible contribution of the LE emission.

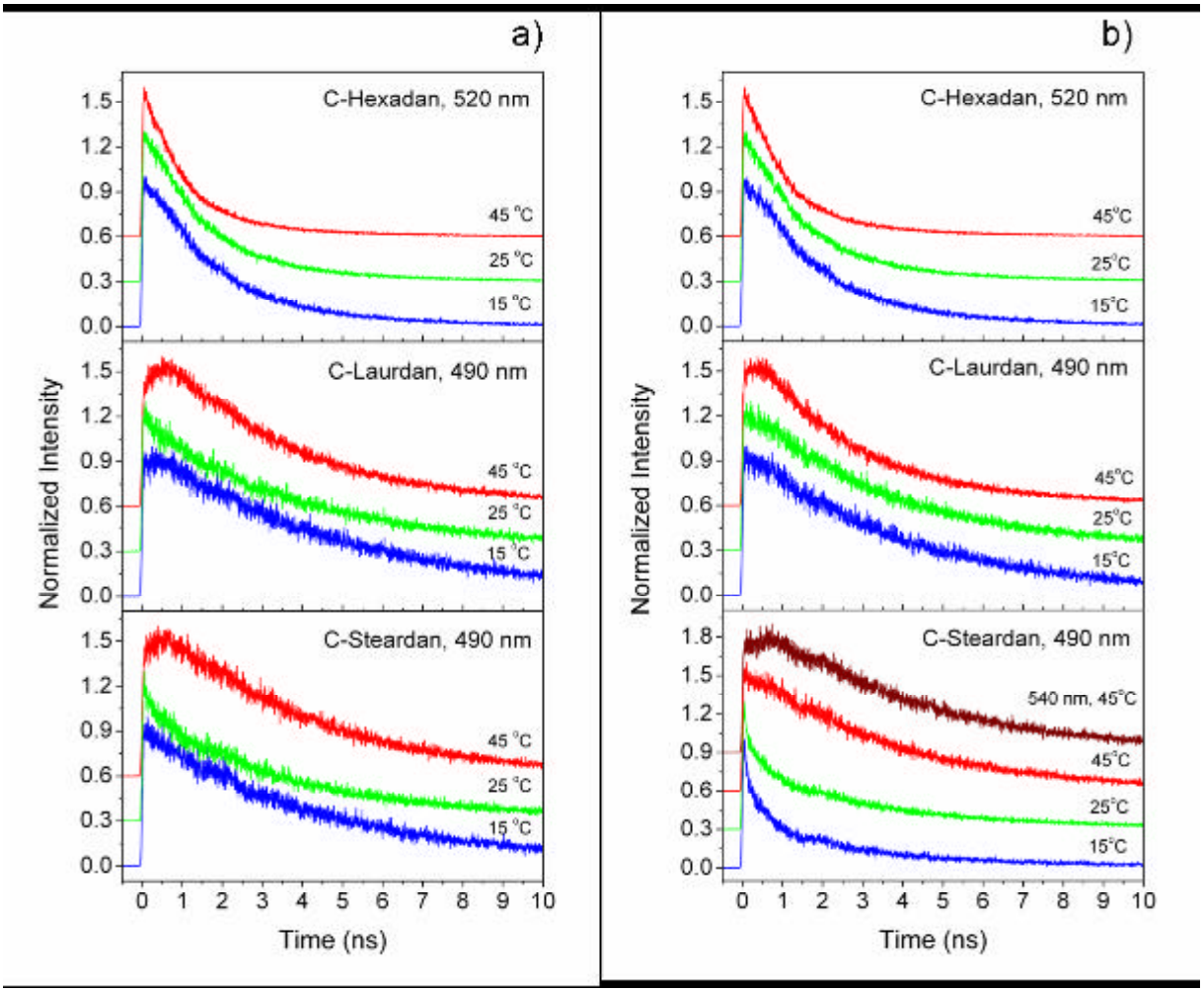

Figure S6. Temperature dependent TRF signals of the CH, CL, and CS in (a) 1:1:1 Raft mixture and (b) 2:2:1 Raft mixture. Excitation wavelength was 380 nm. The curves are displaced in y axis for clarity.

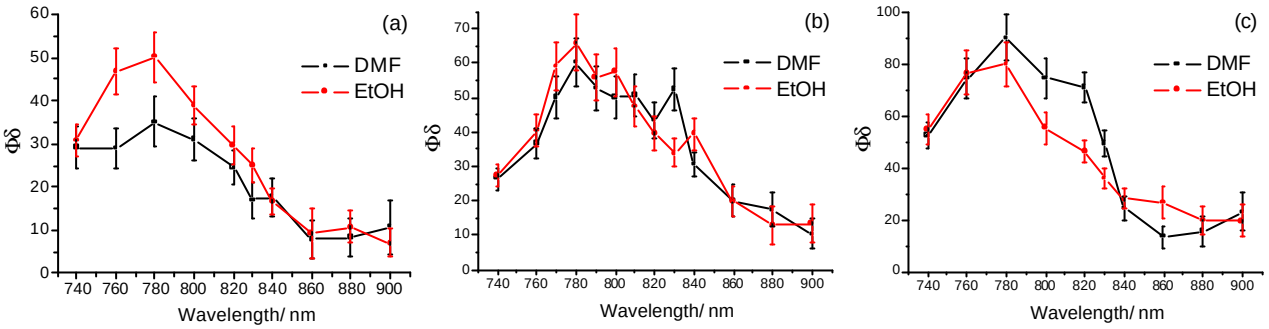

Figure S7. Two-photon action spectra of (a) CH, (b) CL, and (c) CS in DMF (¦) and EtOH (?).

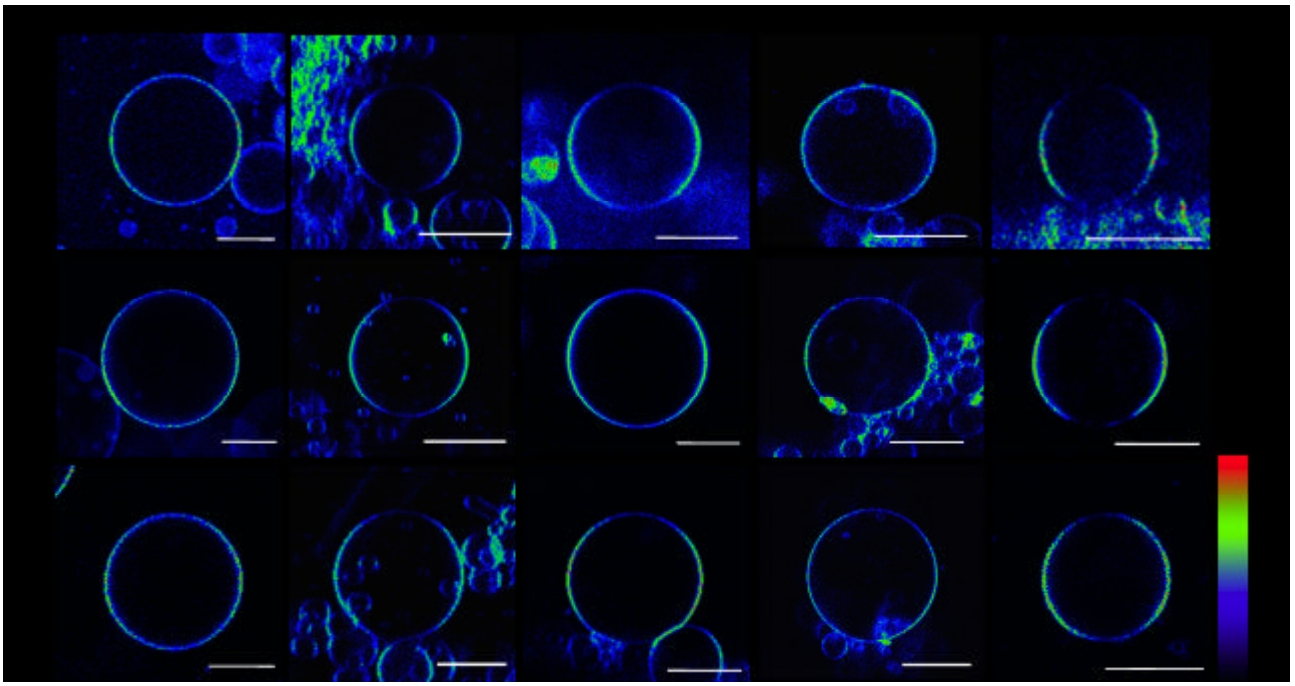

Figure S8. Two-photon fluorescence images of GUVs composed of DOPC, Raft mixture (2:2:1 and 1:1:1), DPPC/chol (chol 40 mol%), and DPPC labeled with CH, CL and CS. The excitation light (λ = 780 nm, I = 200~300 mW/μm^2) was polarized parallel to the horizontal axis of the image.

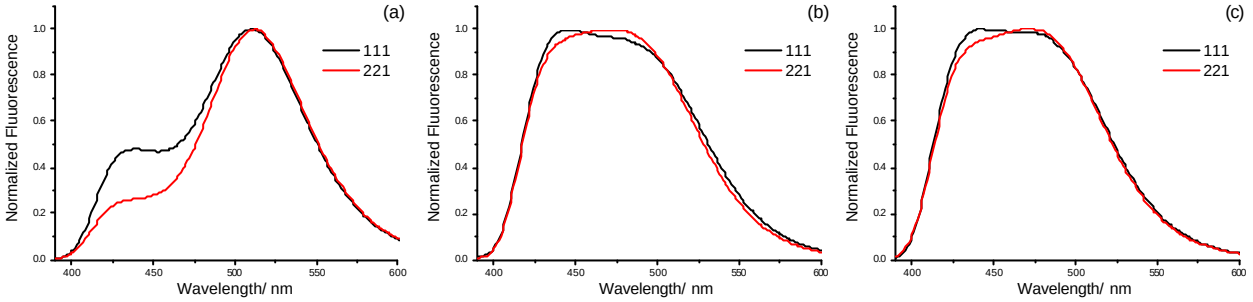

Figure S9. Normalized emission spectra of (a) CH, (b) CL, and (c) CS in the phospholipid vesicles composed of Raft mixture (1:1:1 and 2:2:1) at 25 ± 0.5 °C.

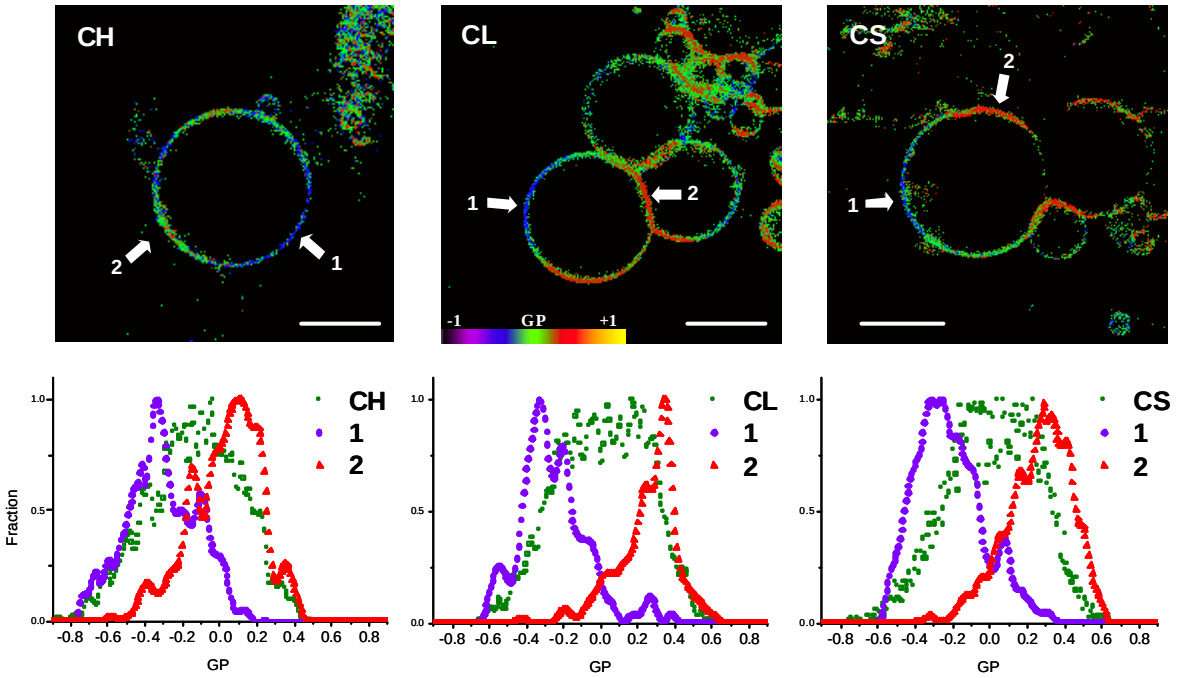

Figure S10. GP images of equatorial section of single GUVs composed of Raft mixture (2:2:1) labeled with CH, CL and CS. Scale bars, 30 μm

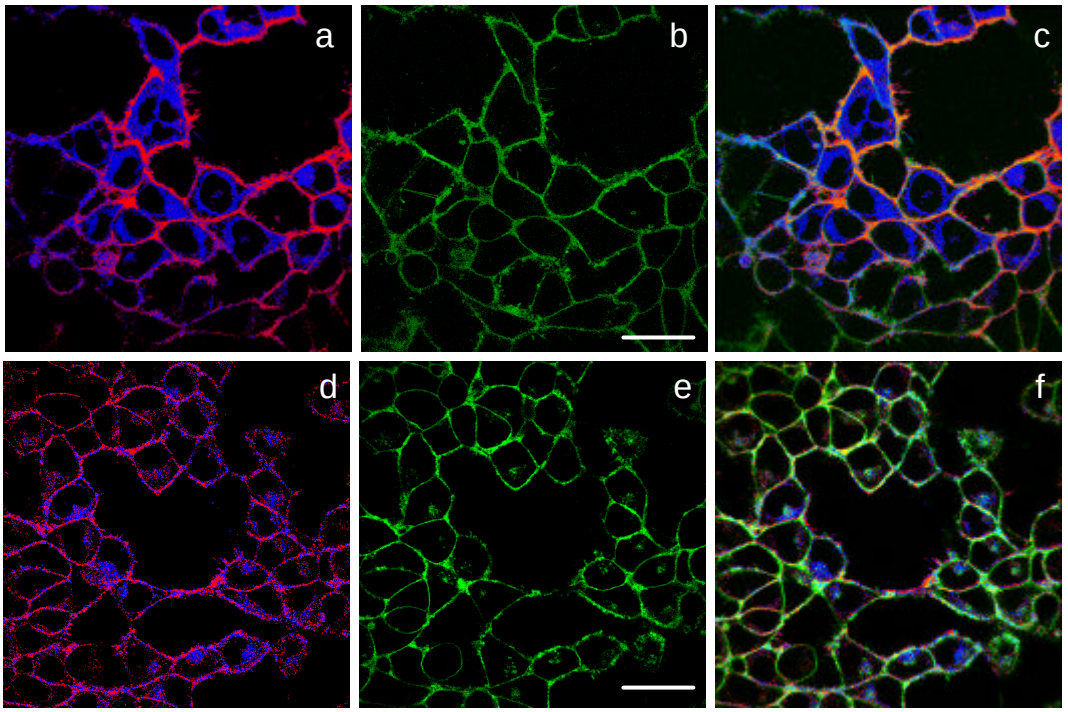

Figure S11. The high GP domains of 293T cells labeled with CL (a) and CS (d), fluorescence image in the same cell labeled with BODIPY-G_{M1} (b, e) and colocalized images (c, f). Scale bar, 30 μm.

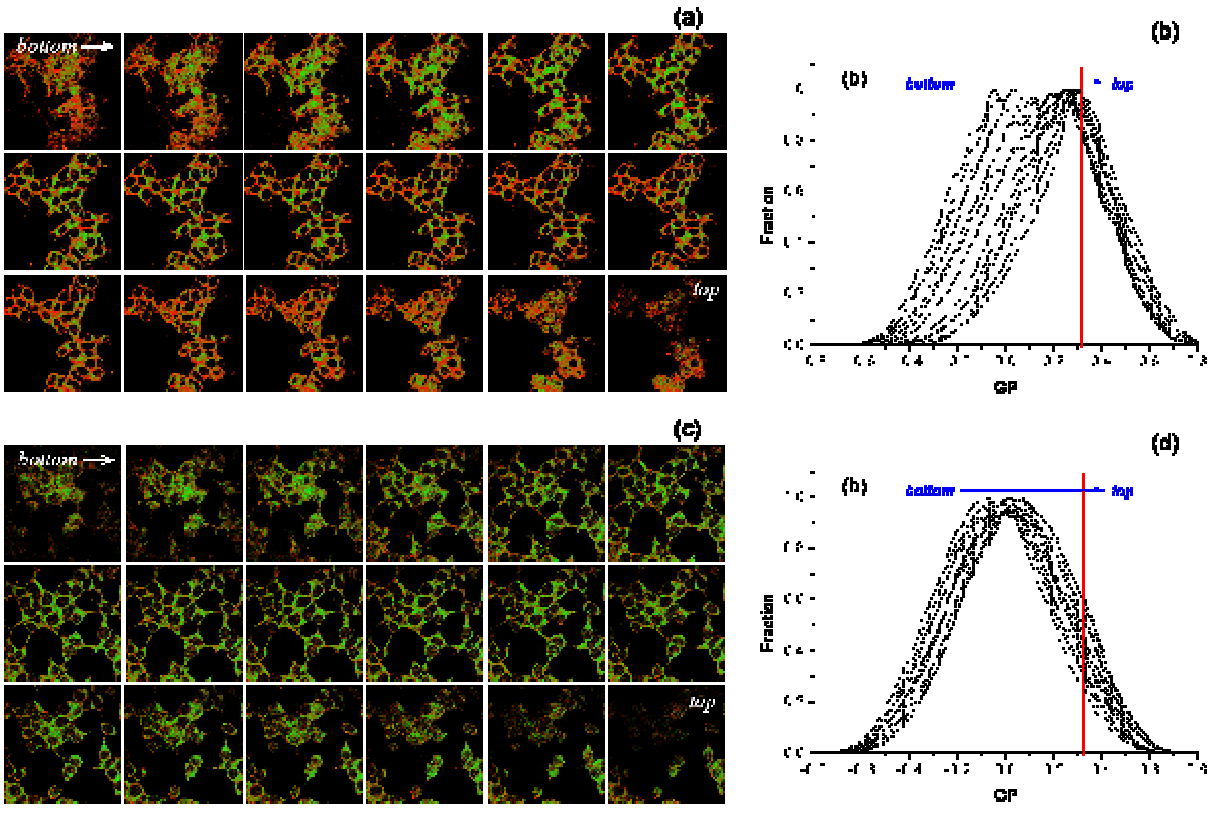

Figure S12. (a, c) Two-photon microscopy images and (b, d) GP distribution curves of each section of CL-stained 293T cell before (a, b) and after (c, d) MβCD treatment. The images were obtained in ~ 0.3 μm increments along the z-direction.

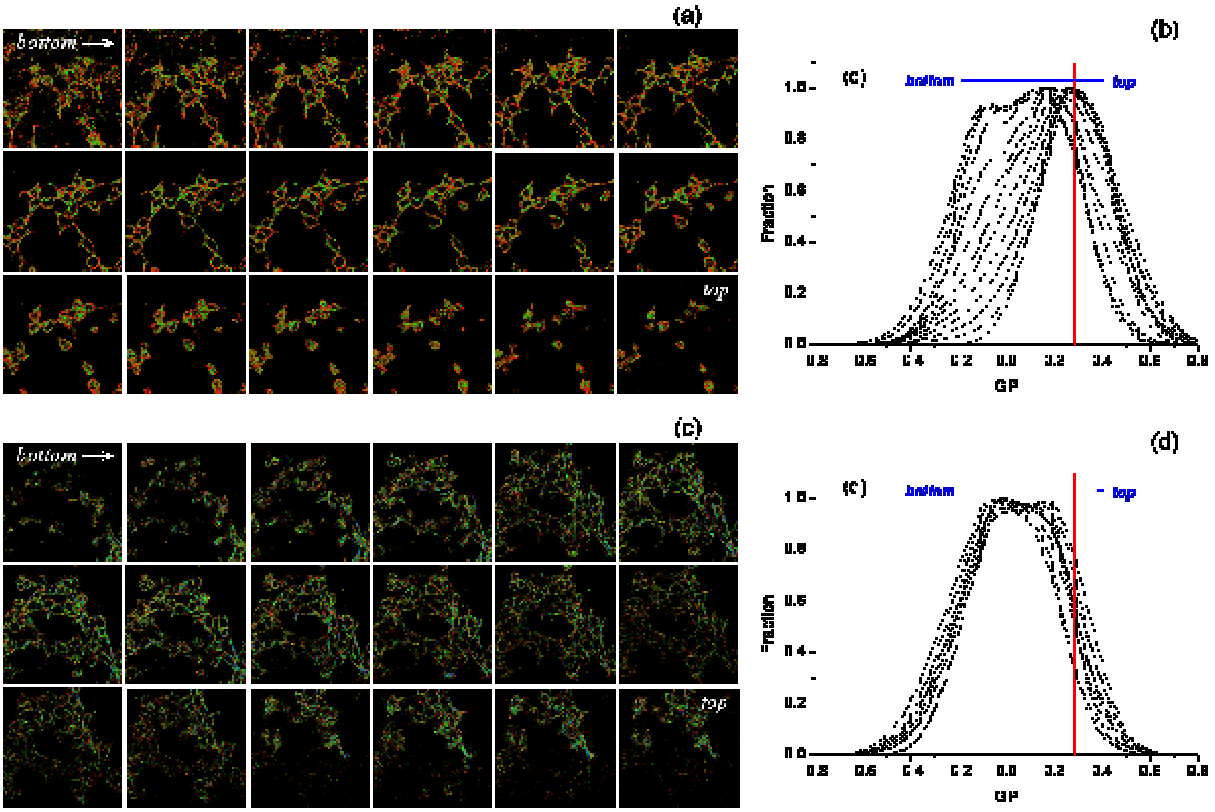

Figure S13. (a, c) Two-photon microscopy images and (b, d) GP distribution curves of each section of CS-stained 293T cell before (a, b) and after (c, d) MβCD treatment. The images were obtained in ~ 0.3 μm increments along the z-direction.